Journal of Alzheimer's Disease Reports 8 (2024) 561–574
DOI 10.3233/ADR-230193
IOS Press

Research Report

Visualization of Microcirculation at Acupoints in vivo of Alzheimer's Disease Animal Model with Photoacoustic Microscope: A Pilot Study

Jing Jiang[a,*], Zidong Wang[a], Ruxia Yu[a], Jiayi Yang[a], Qiucheng Wang[a], Guoqing Wu[a], Yilin Tao[a], Xiaoyue Zhao[a], Yue Wang[a], Zhigang Li[a] and Xiaoqian Qin[b]
[a]*Beijing University of Chinese Medicine, Beijing, China*
[b]*Advantest (China) Co., Ltd. Shanghai, China*

Received 19 December 2023
Accepted 9 February 2024
Published 8 April 2024

Abstract.
Background: Alzheimer's disease may be effectively treated with acupoint-based acupuncture, which is acknowledged globally. However, more research is needed to understand the alterations in acupoints that occur throughout the illness and acupuncture treatment.
Objective: This research investigated the differences in acupoint microcirculation between normal mice and AD animals *in vivo*. This research also examined how acupuncture affected AD animal models and acupoint microcirculation.
Methods: 6-month-old SAMP8 mice were divided into two groups: the AD group and the acupuncture group. Additionally, SAMR1 mice of the same month were included as the normal group. The study involved subjecting a group of mice to 28 consecutive days of acupuncture at the ST36 (*Zusanli*) and CV12 (*Zhongwan*) acupoints. Following this treatment, the Morris water maze test was conducted to assess the mice's learning and memory abilities; the acoustic-resolution photoacoustic microscope (AR-PAM) imaging system was utilized to observe the microcirculation in CV12 acupoint region and head-specific region of each group of mice.
Results: In comparison to the control group, the mice in the AD group exhibited a considerable decline in their learning and memory capabilities ($p < 0.01$). In comparison to the control group, the vascular in the CV12 region and head-specific region in mice from the AD group exhibited a considerable reduction in length, distance, and diameter r ($p < 0.01$). The implementation of acupuncture treatment had the potential to enhance the aforementioned condition to a certain degree.
Conclusions: These findings offered tangible visual evidence that supports the ongoing investigation into the underlying mechanisms of acupuncture's therapeutic effects.

Keywords: Acupuncture, Alzheimer's disease, microcirculation, photoacoustic microscope, senescence-accelerated mouse prone 8

INTRODUCTION

Alzheimer's disease (AD) is the prevailing form of dementia, primarily distinguished by three prominent syndromes: diminished cognitive function [1, 2],

*Correspondence to: Jing Jiang, Beijing University of Chinese Medicine, Beijing 100029, China. E-mail: yingxi7847@126.com.

impaired daily living capacity [3], and mental behavioral abnormalities [4]. These manifestations significantly impact the physical and mental well-being as well as the overall quality of life experienced by affected individuals. Consequently, due to the increasing economic burden on individuals and society at large, AD has emerged as a significant global health concern and social issue, posing a substantial threat to the well-being of populations worldwide [5–10]. The etiology of AD remains incompletely elucidated [11], and the current clinical recommendations advocate for pharmacological interventions that exhibit restricted effectiveness and notable detrimental effects [12–14]. Acupuncture, a therapeutic modality rooted in Chinese medicine, holds significant importance in the management of cognitive, mental, and behavioral disorders [15, 16]. Particularly, it has gained widespread utilization in clinical settings for the treatment of AD. The efficacy of acupuncture therapy is attributed to the particular targeting of acupoints [17, 18]. Although some studies had been conducted to investigate the specificity or sensitization of acupoints [19, 20], most of them focus on *in vitro* pathological sections for observation. However, it is crucial to study the manifestation of specific functions of acupoints *in vivo*.

The photoacoustic microscope (PAM) technique had successfully surpassed the optical "soft limit" and possesses the notable benefit of achieving high imaging resolution [21]. The imaging research conducted at a specific depth under living conditions offers a valuable research platform for investigating the alterations of acupoints in various disorders [22]. Hence, the primary objective of this study was to examine the disparities in the local microcirculation of acupoints between normal mice and AD animal model mice, utilizing an *in vivo* PAM. Additionally, this study aimed to investigate the influence of acupuncture on AD model animals and its consequent effects on the local microcirculation of acupoints. In order to enhance the understanding of acupuncture therapy focused on acupoints, which is imperative to present robust and unbiased visual evidence.

MATERIALS AND METHODS

Animals and ethics statement

The Sibeifu (Beijing) Biotechnology Co., Ltd (animal lot: SCXK (Jing) 2019-0010) provided six-month-old senescence-accelerated mouse prone 8 (SAMP8) and senescence-accelerated mouse resistant 1 (SAMR1) mouse weighing 30.0 ± 2.0 g. The animals were housed in the Animal Experimentation Centre of Beijing University of Chinese Medicine, where they were maintained under controlled conditions. The temperature was kept constant at $24 \pm 2^{\circ}$C, and a 12-h dark/light cycle was implemented. The animals had access to sterile drinking water and were provided with a standard pellet diet ad libitum. Prior to the commencement of the trial, a period of three days was allocated for the acclimatization of all the mice to their respective environments.

The experimental protocol employed in this work was authorized by the Ethics Committee for Animal Experimentation at the Beijing University of Chinese Medicine. The experimental procedures were conducted in accordance with the Animal Research: Reporting of *In Vivo* Experiments (ARRIVE) guidelines and the recommendations of the National Institutes for Animal Research (ID: BUCM-4-2022102001-4022). All researchers involved in this study were certified by the Animal Experimentation Centre at the Beijing University of Chinese Medicine.

Grouping

A total of 21 male mice were included in this study, with 9 mice serving as the normal group (referred to as SAMR1) and 12 mice belonging to the SAMP8 group. The SAMP8 mice were randomly assigned to one of two groups, with 6 mice in each group. The first group was the AD model control group (referred to as the AD group), while the second group received acupuncture treatment (referred to as the Acupuncture group).

Groups intervention

In the Acupuncture group, sterile acupuncture needles (0.25 mm × 2.5 mm; *Beijing Zhongyan Taihe Medicine* Company) were inserted transversely to a depth of 2.5 mm at the ST-36 (Zusanli) and CV12 (Zhongwan) acupuncture points, as seen in Fig. 1. The acupoints were subjected to a daily intervention of 20 min, wherein the needles were affixed using tape. This continuous intervention was carried out for a duration of 28 days. Both the normal and AD groups of mice were subjected to a 20-min immobilization period, similar to the Acupuncture group, only without the administration of acupuncture.

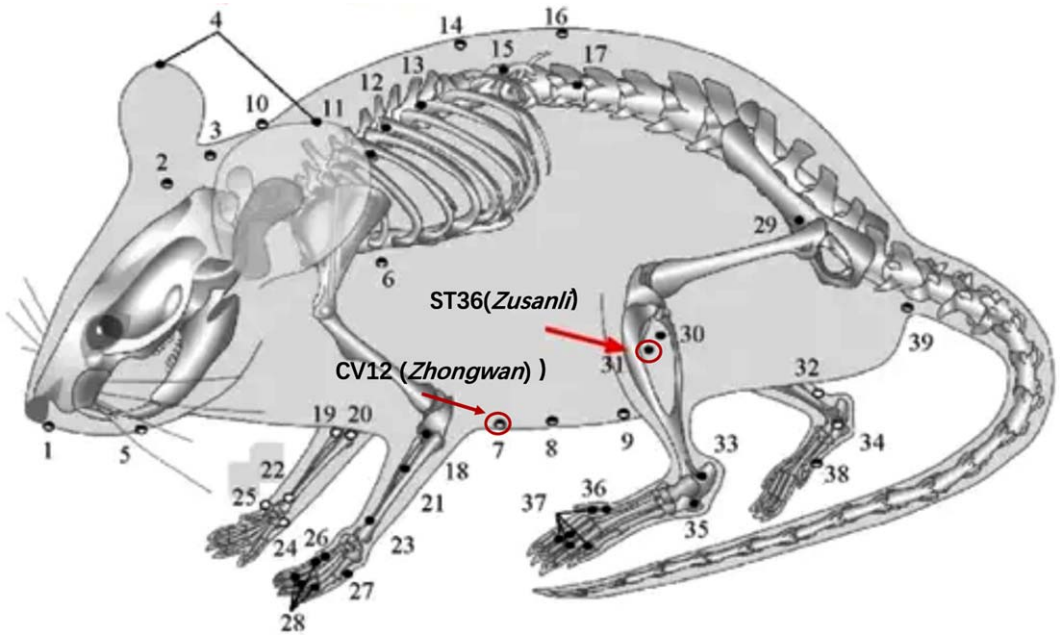

Fig. 1. Selected acupoints on the mouse (ST36 and CV12).

Morris water maze test

Following a 28-day intervention period, the mice from each experimental group underwent evaluation using the Morris water maze. The experimental apparatus utilized in this study was the Morris water maze, which comprised a circular tank with a diameter of 120 cm and a height of 50 cm. The tank was filled with opaque water, which was made non-transparent by the addition of black ink, reaching a depth of 30 cm. Data collection was conducted using a TOTA-450d video camera, manufactured in Japan, which was securely mounted on the ceiling. The camera was connected to a video recorder equipped with an automated tracking system, manufactured by *Daheng* Group in China. This setup allowed for the automatic collection of data. A detachable platform with a diameter of 9.5 cm and a height of 30 cm was positioned within the pool, specifically in quadrant III. The pool area was conceptually partitioned into four quadrants (I, II, III, and IV) of equivalent dimensions. Distinctive visual stimuli in various geometric forms were strategically positioned on the inside surface of each quadrant of the tank, ensuring their conspicuousness to the mice.

The hidden platform trial was employed to assess the cognitive capabilities of the mice. All experimental subjects, in this case mice, underwent training in the Morris water maze task, which involved locating a concealed platform. The entrance locations selected were Quadrant I, Quadrant II, and Quadrant IV. Every individual mouse was released from three distinct starting positions and given a time limit of 60 s to locate the concealed platform. The escape latency of three trials was recorded and the average value was calculated.

The memory capacity of the mice was assessed using a spatial probing trial. The removal of the platform occurred on the day subsequent to the conclusion of the hidden platform trial. Each mouse was subjected to a single 60-s trial in the pool, commencing from the identical initial location employed in the concealed platform experiment. The time it took for the platform to cross was measured and recorded during the experiment.

Photoacoustic scope imaging

The photoacoustic imaging equipment, namely the Hadatomo TM Z WEL5200 model, was generously provided by Advantest (China) Co., Ltd. The system comprised a PA transmitter/receiver unit integrated with a laser optical fiber positioned at the core of an annular array transducer. Additionally, an XY stage was incorporated to enable mechanical two-dimensional scanning within an imaging field.

Fig. 2. The Hadatomo TM Z WEL5200 photoacoustic imaging system (supported by the Advantest (China) Co., Ltd).

Furthermore, a control and signal processing unit were included for system operation and data analysis.

The annular array transducer had a concave surface with a geometric focus of 6 mm and a center hole (1 mm) for the laser outlet. The concave geometry was divided into four ring-shaped PZT elements (a center frequency of 60 MHz ± 20%) with a minimum diameter of 1 mm and a maximum diameter of 6 mm. The Nd:YAG laser was selected to irradiate 532 nm pulsed beams at a repetition rate of 1 kHz and a pulse width of 1.2 ns. The emitted pulse energy was measured to be 16 μ J pulse. While the PA transmitter/receiver unit was raster-scanned by the XY stage, an event of emitting a laser pulse and receiving PA signals was repeatedly performed to acquire the three-dimensional distribution of the optical absorbers in the imaging field. In each receiving event, the PA waves generated at the object by the laser irradiation were received by each element of the annular array transducer and recorded at a sampling frequency of 500 MHz (Fig. 2).

The experimental animals (21 mice from each group) were anesthetized with isoflurane gas (using a concentration of 2.5% during induction anesthesia and maintaining a concentration of 2%) for skin preparation. Hair was removed from the abdominal CV12 (*Zhongwan*) acupoint region and the head region with depilatory cream (Fig. 3). After skin preparation, the animals were anesthetized with gas for 30 min before undergoing photoacoustic imaging scanning. Continuous anesthesia during the scanning process. Following the completion of the scan, the Euclid R2.00 software (developed by Adventure Co., Ltd.) was employed to quantify and gather image and microcirculation data pertaining to the region of interest (ROI) measuring 6 mm × 6 mm × 6 mm (as depicted in Fig. 3). This included the measurement of vascular characteristics such as length (in

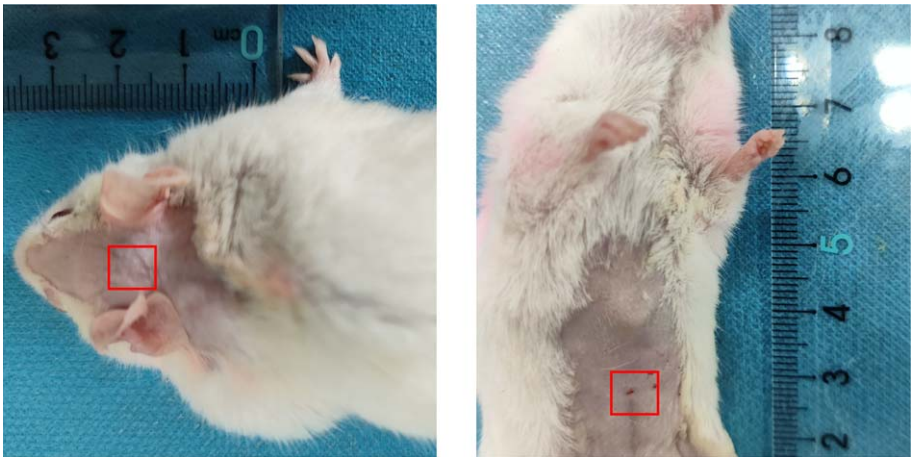

Fig. 3. Regions of interested selected on the mice (Left: the head region, Right: CV12 (*Zhongwan*) acupoint region, 6mm × 6 mm).

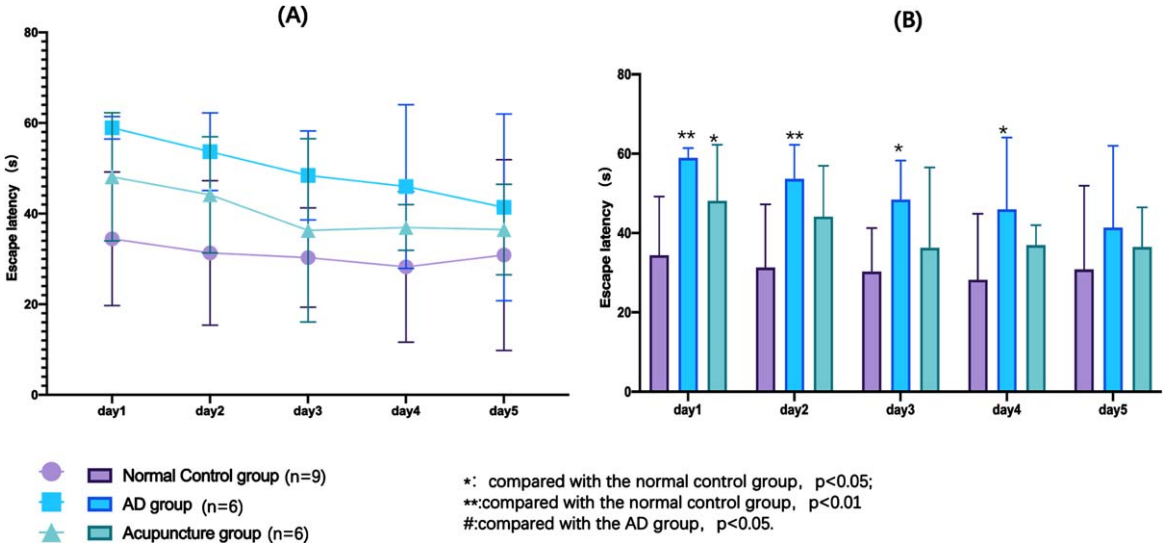

Fig. 4. Results of hidden platform trial in the Morris water maze test. A) The changes of escape latency with the training days of each group. B) The differences of each group during each training days.

millimeters), distance (in millimeters), sinuosity, and diameter (in millimeters) within the specified regions.

Statistical analysis

The Statistical Package for the Social Sciences (SPSS) version 25.0 (SPSS, Inc., Chicago, IL, USA) was used to conduct statistical analyses, and data were reported as means ± standard deviation. For all comparisons, the significance threshold was set at 0.05. Multivariate analysis of variance (ANOVA) with repeated measures was used for the general linear model using the SPSS software, and pairwise comparison was used for different groups and different measurement times. Mauchly's test of sphericity was used to assess whether there were relations among the repeatedly measured data. The One-way ANOVA statistical test was employed to analyze the variations among the Normal, AD, and acupuncture groups for each dataset. The application of Pearson correlation analysis was employed to examine the relationship between microcirculation data of acupoints and the head.

RESULTS

Acupuncture could improve the spatial learning and memory ability of SAMP8 mice

The escape latency of hidden platform trial could reflect the spatial learning ability of the experimental animals. As we could see from the Fig. 4, the escape latency was shortened with the training days increased. The normal group performed best of the three groups ($p < 0.05$). What's more, the acupuncture group performed better than the AD group (Fig. 4A). Especially, at the first day of training, the acupuncture group performed significantly better than the AD group (Fig. 4B). Notably, at the last day of training, the escape latency of normal group was a little bit of longer than the fourth day and there were no significantly differences of the three groups. We assumed that might be the training fatigue of mice.

The times of crossing the platform region in the probe trial could reflect the spatial memory ability of the experimental animals. More times of crossing the platform region, better the memory ability of the animal has. In the Fig. 5A, the times of crossing the platform region of normal group was significantly more than AD and acupuncture group (compared with AD group, $p < 0.01$; compared with acupuncture group, $p < 0.05$), and acupuncture group was also more than AD group ($p < 0.01$). Figure 5B showed the search strategy, which was an indicator that measure the analytical and problem-solving abilities of animals. As showed in Fig. 5B, the search strategy of normal group was more likely linear based type, AD group was belonged to edge type and acupuncture group was belonged to trend type. The search strategy of dementia animals may undergo abnormal changes. For example, there are only edge type to random type, or random type to

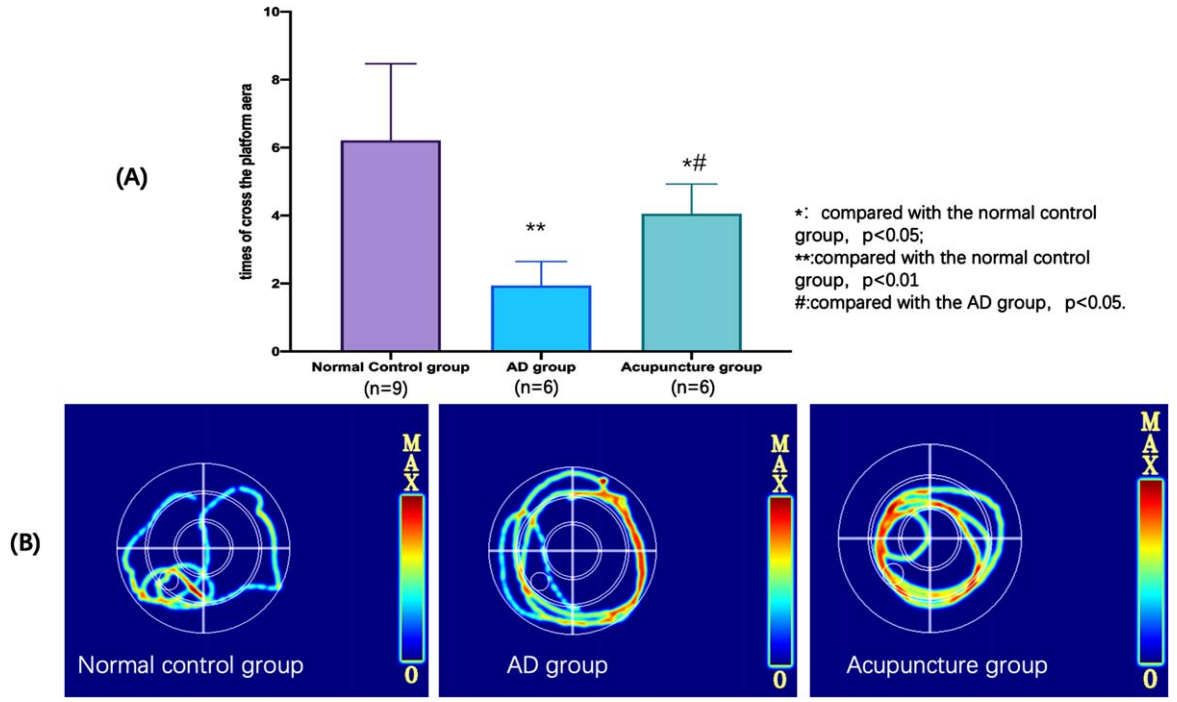

Fig. 5. Results of spatial probe trial in the Morris water maze test. A) The differences of the times of crossing the platform region of each group in the spatial probe trial. B) The search strategy of each group in the spatial probe trial.

edge type, and trend type and linear type are relatively rare.

The above results illustrated two points, one was the SAMR1 mice (normal group) had a better learning and memory ability than SAMP8 mice (AD group), the other was acupuncture treatment at the acupoint ST36 and CV12 could improve the leaning and memory ability of SAMP8 mice to a certain extent.

Differences between SAMP8 and SAMR1 mice at the selected acupoint region in photoacoustic imaging and effects of acupuncture on microcirculation of SAMP8 mice

The top view of the photoacoustic imaging of CV12 acupoint region of each group was showed in the Fig. 6 (6 mm × 6 mm). As observed, the CV12 acupoint region exhibited the highest vascular density and hemoglobin density in the normal group, accompanied by the most intricate structure and branches. Conversely, the aforementioned markers among the AD group had the lowest values. Furthermore, it was observed that the acupuncture group had higher levels of vascular density and hemoglobin density compared to the AD group.

Euclid R2.00 (Adventure Co., Ltd.) could extract the vascular feature from the original photoacoustic image by analyzing the vascular skeleton (centerline) and noise removal (Fig. 7A). Euclid R2.00 could also collect the microcirculation data of the region of CV12 acupoint including the length (mm), distance (mm), sinuosity, and diameter (mm) of vascular in the regions. We found the length, distance and diameter of this region in the normal group were significantly higher than AD group (at length and distance, $p < 0.01$; at diameter, $p < 0.05$). Meanwhile, the length and distance of this region in the acupuncture group were also significantly higher than AD group ($p < 0.05$). However, there was no significantly difference in the sinuosity of this region in the three groups (Fig. 7B-D).

Differences between SAMP8 and SAMR1 mice at the head region in photoacoustic imaging and effects of acupuncture on microcirculation of SAMP8 mice

The top view of the photoacoustic imaging of head region of each group was showed in the Fig. 8 (6 mm × 6 mm). As we all seen, the within the head region in normal group, the vascular density and

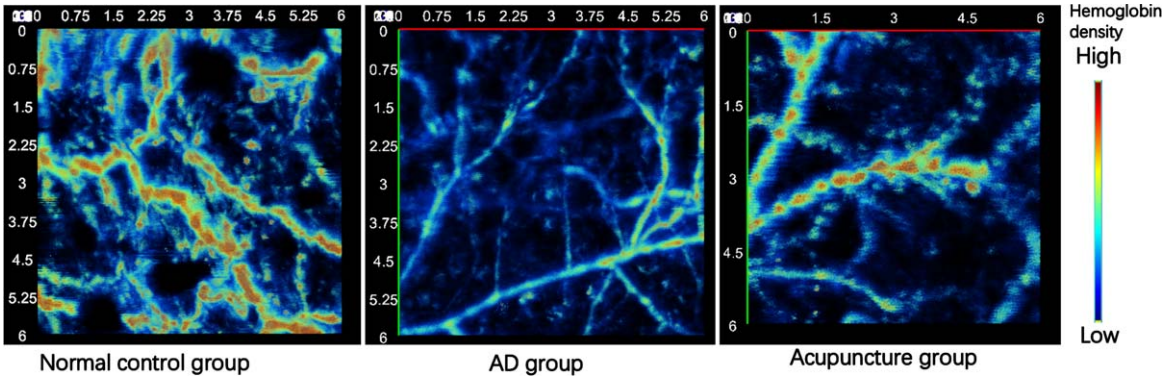

Fig. 6. The top view of photoacoustic images of CV12 acupoint region of each group (6 mm × 6 mm).

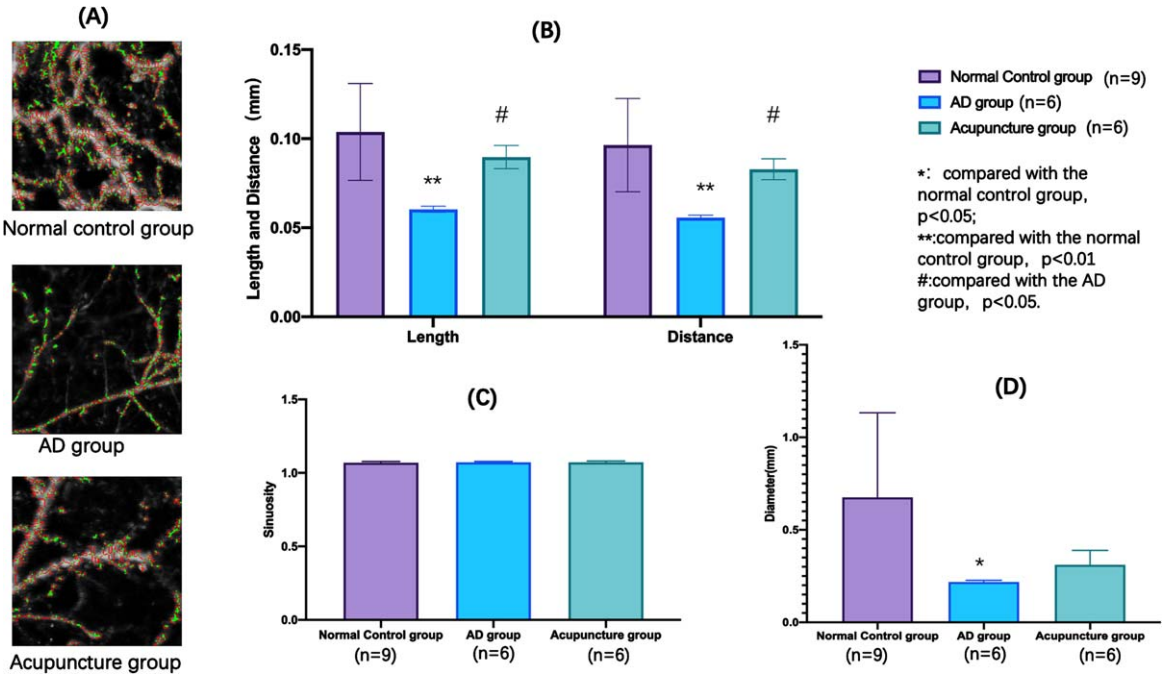

Fig. 7. Microcirculation differences at CV12 acupoint region of each group.

hemoglobin density were highest and the structure and branches were the most complex. On the contrary, the above indicators in the AD group were all the lowest. Moreover, in acupuncture group the vascular density and hemoglobin density were higher than AD group.

We found the length and distance of the head region in the normal group were significantly higher than AD group ($p < 0.05$). Meanwhile, the length and distance of this region in the acupuncture group were also significantly higher than AD group ($p < 0.05$). However, there was no significant difference in the sinuosity and diameter of this region in the three groups (Fig. 9B-D).

We used correlation analysis to explore the relation between the head region and the CV12 acupoint region, as illustrated in Fig. 10. These findings revealed that the length of vascular in the CV12 acupoint region had a significant correlation with the length of vascular in the head region ($r = 0.75$, $R2 = 0.56$, $p < 0.01$, Fig. 10A). Similarly, the distance of vascular in the CV12 acupoint region also had a significant correlation with the distance of vascular in the head region ($r = 0.82$, $R2 = 0.67$, $p < 0.01$, Fig. 10B).

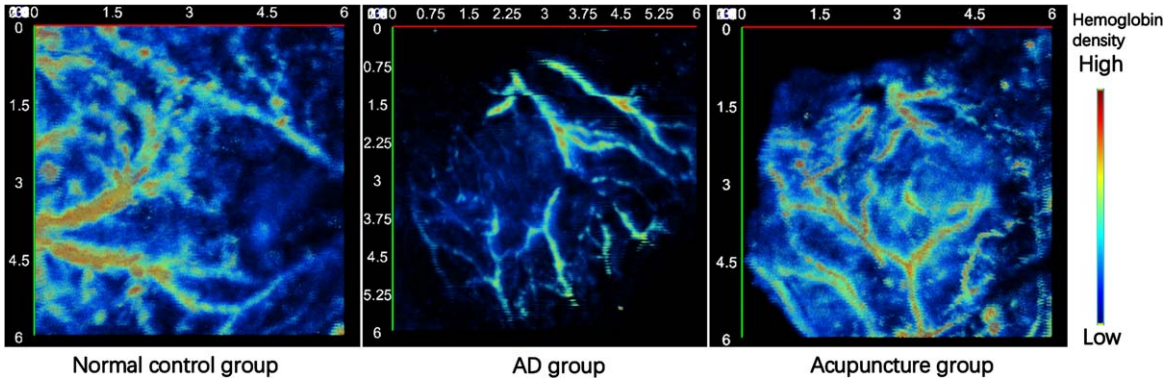

Fig. 8. The top view of photoacoustic images of the head region of each group (6 mm × 6 mm).

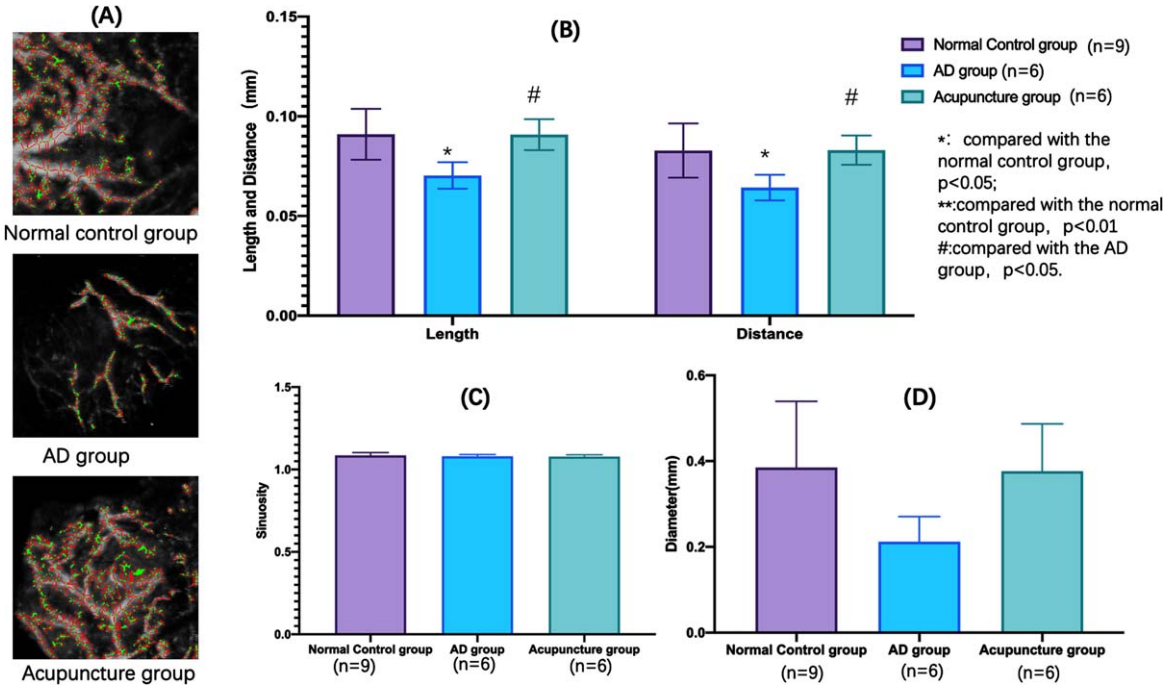

Fig. 9. Microcirculation differences at the head region of each group.

DISCUSSION

Currently, there is ongoing research that is continuously advancing our understanding of the mechanism of acupuncture intervenes in AD. The current body of reviews indicated that the combination of acupuncture and medicine yielded more benefits for people with AD in comparison to the use of medication alone [15, 23–28]. In the realm of animal experimentation, numerous research had been conducted to investigate the presence of acupuncture intervention in AD through diverse mechanisms [29], including to alterations in synaptic morphology and structure by regulation of some relevance protein expression [30, 31], mitigation of Aβ deposition [32, 33] and excessive tau protein phosphorylation [34–37], inhibition of central nervous system inflammation and neuronal apoptosis [38–40], and resistance against oxidative stress [41, 42]. Acupuncture is an intervention based on acupoints, and multiple literature studies on the selection of acupoints for AD acupuncture intervention have found that ST36 (*Zusanli*) and CV12 (*Zhongwan*) acupoints were one of the more commonly used acupoints in AD acupuncture intervention [28]. For the intervention in this research, we specifically selected bilateral ST36 and

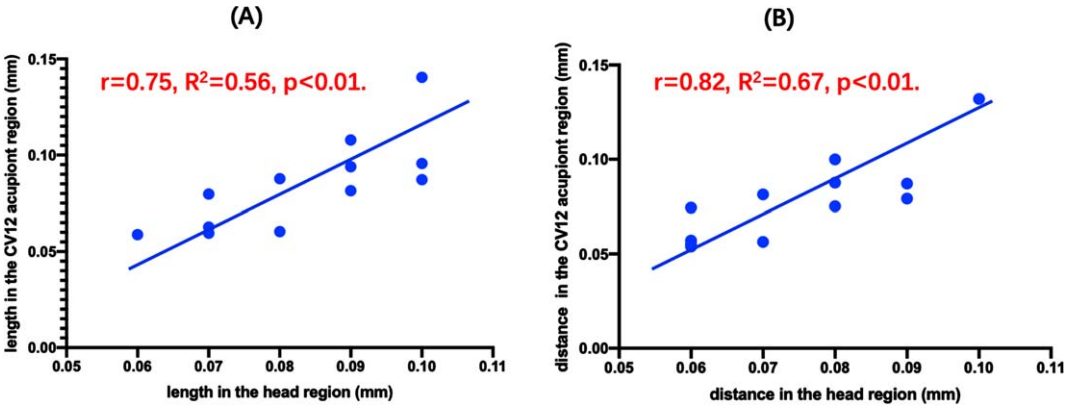

Fig. 10. Relation of matriculation data between the head region and the CV12 acupoint region.

CV12 acupoints. The primary selection criteria were based on the extensive clinical research on acupuncture intervention, which had consistently shown that stimulating the ST36 acupoint might significantly improve the clinical symptoms of patients with AD [43]. Furthermore, animal experiments have demonstrated that the ST36 acupoint could enhance the cognitive functions and slow down the progression of the central nervous system in animal models of AD. This was achieved through the activation of various signaling pathways such as TLR4/NF kB [44, 45], JNK [46], melatonin [47], RhoA/ROCK [48], and P38 [49], with a particular emphasis on restoring the balance of gut microbiota [46, 50, 51]. Simultaneously, our team has discovered, via several prior experimental investigations, that acupuncture could enhance the cognitive functions of SAMP8 mice by rectifying the dysbiosis of gut microbiota [52]. Hence, in this study, drawing from traditional Chinese medicine theory, we chose the acupoints, ST36 and CV12, which were most closely associated with regulating intestine function, for our intervention. Through the examination of the brain's microcirculation, we aim to uncover the precise influence and consequences of acupuncture intervention on the central nervous system. In addition, we also found that the GV20 (*Baihui*) acupoint region, situated at the apex of the mouse's head, was frequently selected as a target for intervention in cases of AD [53, 54]. According to the acupoint sensitization hypothesis, acupoints serve as the points where diseases manifest and are also the specific areas targeted for therapy [55, 56]. Can manipulating the ST36 and CV12, which impact the microbiota's function, lead to alterations in microcirculation within certain regions of the head? To investigate the correlation between the peripheral and central areas, we specifically chose the head region as the focal point for observing photoacoustic imaging in this investigation.

Biomedical imaging technology had a significant role and finds extensive used in the field of medicine [22, 57]. It facilitated the differentiation between healthy and sick tissues by analyzing the biological information present in biological tissues, including but not limited to hemoglobin [58, 59], melanin [60], bilirubin [61], lipids [62–64], and water [65]. The spatial arrangement of this biological data inside the organism was indicative of the tissue's functionality and pathological condition. A more in-depth examination of this data might provide significant foundational knowledge for the timely identification, intermediate therapeutic evaluation, and ultimate treatment results of many diseases within the field of biomedical sciences [66, 67].

Photoacoustic microscopy (PAM) technology offered enhanced imaging resolution for biological applications, although at the expense of reduced penetration depth [22]. The photoacoustic signal of a photoacoustic microscopy imaging system is generated at the point where the light and sound focal points overlap. Therefore, photoacoustic microscopy imaging systems are usually divided into two types based on the type of focal point: acoustic resolution PAM (AR-PAM) and optical resolution PAM (OR-PAM) [68]. In the above two systems, AR-PAM has explored various biomedical information [69], such as microvascular networks and internal organ structure imaging in anatomical imaging, oxygen saturation, hemodynamic processes, and vasodilation in functional imaging, and has also conducted many

studies in fields such as cardiovascular disease [59, 70, 71], cerebrovascular disease [72–76], dermatology [77–79], and oncology [80–83].

Although a series of studies have been carried out around photoacoustic imaging technology, few studies have applied this technology to the study of acupoints. In the early stage of our research project, photoacoustic imaging technology was used to explore the local vascular structure of ST36 and GB34 in the mouse model of knee osteoarthritis [84]. However, because there was a certain degree of overlap between the modeling site of knee osteoarthritis and the observation area of interest of photoacoustic imaging. In this study, we selected SAMP8 mice, an AD animal model without surgical modeling, to observe the local microcirculation of its specific acupoint, and to observe the effect of acupuncture intervention on the local microcirculation of specific acupoint region.

The results of this experiment demonstrate a notable difference in the microcirculation organization of the CV12 region between SAMP8 mice and SAMR1 mice. The measurements of vascular length, distance, and diameter in the abdomen CV12 region of SAMP8 mice, aged 7-month (28 days post-intervention at 6-month), shown a statistically significant reduction compared to those of SAMR1 mice The findings of this study might partially validate our prior research findings about the intestinal microbiota of SAMP8 mice [52]. It was noteworthy that SAMP8 mice also exhibits an imbalance in their intestinal microbiota, which was positively associated with the deterioration of cognitive functions, namely learning and memory abilities. Simultaneously, it was observed that the vascular length and distance in the abdomen CV12 region exhibited a significant degree of enhancement after a 28-day consecutive acupuncture treatment at CV12. Further experimentation will be required to ascertain if this alteration in structure has the potential to induce modifications in both the structure and functionality of the gut microbiota. Furthermore, within the scope of this investigation, we also conducted observations on the microcirculation at the designated region of head, which served as a control site devoid of any acupuncture intervention. The research findings indicated a significant reduction in the vascular length and distance of the head region of SAMP8 mice compared to SAMR1. Furthermore, a positive correlation was observed between the vascular length and distance in the head and those in the abdominal CV12 region. This offered the opportunity to assess the cerebral microcirculation by examining the alterations in microcirculation of related acupoints. However, for a more precise understanding of the cerebral microcirculation, it might be necessary to investigate the imaging of brain microcirculation in model animals after craniotomy in later experimental investigations. It is important to acknowledge that prolonged acupuncture treatment may lead to notable alterations in cerebral microcirculation. However, the precise mechanisms behind these changes need additional investigation.

While this study had yielded some promising findings via the use of photoacoustic imaging technology, it was important to acknowledge that there were still several limitations within the scope of the experimental investigation. The imaging platform used in this study was the AR-PAM. Furthermore, it is worth considering the potential integration of a multi-wavelength OR-PAM imaging system in further study. This innovative approach might have promise for uncovering a greater depth of microcirculation information. Moreover, this study only analyzed the local microcirculation of the CV12 region after acupuncture intervention, whereas the ST36 region was not included in the analysis. One of the operational rationales was to the diminutive size of the ST36 region in mice, which was significantly impacted by the presence of subcutaneous bones. In this experiment, the imaging depth of photoacoustic imaging is 6 mm. In the ST36 acupoint region of mice, the imaging depth of 6 mm was affected by local tibia, resulting in a large amount of noise in the image, making it impossible to conduct statistical analysis. Therefore, when analyzing the local microcirculation data of acupoints, we have to abandon the statistical analysis of photoacoustic imaging data in the ST36 acupoint region. For future investigations, we will use rats or rabbits as the experimental subjects for AD models. This choice will enable us to get a more comprehensive understanding of the microcirculation information in each acupoint location during the progression of the illness.

Conclusion

This work used AR-PAM to investigate the microcirculation of the CV12 region and the head region in SAMP8 and SAMR1 mice. Significantly, a conspicuous discrepancy was detected between the two kinds of mice. Concurrently, we have shown the influence of acupuncture intervention on the microcirculation of the CV12 region and the head region in

SAMP8 mice. The present research provided visual data that might be used to further investigate the impacts and mechanisms of acupuncture intervention in AD. In subsequent research, the focus will consistently be on observing the modifications of specific acupoints, while simultaneously exploring the fundamental mechanisms via which acupuncture intervention influences AD.

AUTHOR CONTRIBUTIONS

Jing Jiang (Conceptualization; Funding acquisition; Writing – original draft; Writing – review & editing); Zidong Wang (Data curation); Ruxia Yu (Data curation); Jiayi Yang (Data curation); Qiucheng Wang (Data curation); Guoqing Wu (Data curation); Yilin Tao (Data curation); Xiaoyue Zhao (Data curation); Yue Wang (Data curation); Zhigang Li (Supervision); Xiaoqian Qin (Software; Visualization).

ACKNOWLEDGMENTS

The authors have no acknowledgements to report.

FUNDING

This study was supported by National Natural Science Foundation of China (grant No. 82174515).

CONFLICT OF INTEREST

The authors have no conflict of intertest to report.

DATA AVAILABILITY

The data that support the findings of this study are available on request from the corresponding author, Jing Jiang, upon reasonable request.

REFERENCES

[1] Studart AN, Nitrini R (2016) Subjective cognitive decline: The first clinical manifestation of Alzheimer's disease? *Dement Neuropsychol* **10**, 170-177.

[2] Wang X, Huang W, Su L, Xing Y, Jessen F, Sun Y, Shu N, Han Y (2020) Neuroimaging advances regarding subjective cognitive decline in preclinical Alzheimer's disease. *Mol Neurodegener* **15**, 55.

[3] Jia J, Xu J, Liu J, Wang Y, Wang Y, Cao Y, Guo Q, Qu Q, Wei C, Wei W, Zhang J, Yu E (2021) Comprehensive management of daily living activities, behavioral and psychological symptoms, and cognitive function in patients with Alzheimer's disease: A Chinese consensus on the comprehensive management of Alzheimer's disease. *Neurosci Bull* **37**, 1025-1038.

[4] Huang YY, Gan YH, Yang L, Cheng W, Yu JT (2023) Depression in Alzheimer's disease: Epidemiology, mechanisms, and treatment. *Biol Psychiatry*, doi: 10.1016/j.biopsych.2023.10.008

[5] Clay E, Zhou J, Yi ZM, Zhai S, Toumi M (2019) Economic burden for Alzheimer's disease in China from 2010 to 2050: A modelling study. *J Mark Access Health Policy* **7**, 1667195.

[6] Ikeda S, Mimura M, Ikeda M, Wada-Isoe K, Azuma M, Inoue S, Tomita K (2021) Economic burden of Alzheimer's disease dementia in Japan. *J Alzheimers Dis* **81**, 309-319.

[7] Nandi A, Counts N, Chen S, Seligman B, Tortorice D, Vigo D, Bloom DE (2022) Global and regional projections of the economic burden of Alzheimer's disease and related dementias from 2019 to 2050: A value of statistical life approach. *EClinicalMedicine* **51**, 101580.

[8] Szabo S, Lakzadeh P, Cline S, Palma Dos Reis R, Petrella R (2019) The clinical and economic burden among caregivers of patients with Alzheimer's disease in Canada. *Int J Geriatr Psychiatry* **34**, 1677-1688.

[9] Tahami Monfared AA, Byrnes MJ, White LA, Zhang Q (2022) The humanistic and economic burden of Alzheimer's disease. *Neurol Ther* **11**, 525-551.

[10] Yang Z, Levey A (2015) Gender differences: A lifetime analysis of the economic burden of Alzheimer's disease. *Womens Health Issues* **25**, 436-440.

[11] Zhang C (2023) Etiology of Alzheimer's disease. *Discov Med* **35**, 757-776.

[12] Abbate C (2022) Research on Alzheimer's syndromes is critical to improve diagnosis, patient management and non-pharmacological treatments, but is under-pursued. *Front Aging Neurosci* **14**, 1039899.

[13] Dafre R, Wasnik P, Sr. (2023) Current diagnostic and treatment methods of Alzheimer's disease: A narrative review. *Cureus* **15**, e45649.

[14] Devi G (2023) A how-to guide for a precision medicine approach to the diagnosis and treatment of Alzheimer's disease. *Front Aging Neurosci* **15**, 1213968.

[15] Wang XS, Li JJ, Wang YS, Yu CC, He C, Huang ZS, Jiang T, Hao Q, Kong LH (2021) Acupuncture and related therapies for the cognitive function of Alzheimer's disease: A network meta-analysis. *Iran J Public Health* **50**, 2411-2426.

[16] WuLi W, Harn HJ, Chiou TW, Lin SZ (2021) Chinese herbs and acupuncture to improve cognitive function in Alzheimer's disease. *Tzu Chi Med J* **33**, 122-127.

[17] Li N, Guo Y, Gong Y, Zhang Y, Fan W, Yao K, Chen Z, Dou B, Lin X, Chen B, Chen Z, Xu Z, Lyu Z (2021) The anti-inflammatory actions and mechanisms of acupuncture from acupoint to target organs via neuro-immune regulation. *J Inflamm Res* **14**, 7191-7224.

[18] Tan H, Tumilty S, Chapple C, Liu L, McDonough S, Yin H, Yu S, Baxter GD (2019) Understanding acupoint sensitization: A narrative review on phenomena, potential mechanism, and clinical application. *Evid Based Complement Alternat Med* **2019**, 6064358.

[19] Ding N, Jiang J, Qin P, Wang Q, Hu J, Li Z (2018) Mast cells are important regulator of acupoint sensitization via the secretion of tryptase, 5-hydroxytryptamine, and histamine. *PLoS One* **13**, e0194022.

[20] Li W, Liu J, Chen A, Dai D, Zhao T, Liu Q, Song J, Xiong L, Gao XF (2022) Shared nociceptive dorsal root ganglion neurons participating in acupoint sensitization. *Front Mol Neurosci* **15**, 974007.

[21] Sathiyamoorthy K, Strohm EM, Kolios MC (2017) Low-power noncontact photoacoustic microscope for bioimaging applications. *J Biomed Opt* **22**, 46001.

[22] Neprokin A, Broadway C, Myllylä T, Bykov A, Meglinski I (2022) Photoacoustic imaging in biomedicine and life sciences. *Life (Basel)* **12**, 588.

[23] Du K, Yang S, Wang J, Zhu G (2022) Acupuncture interventions for Alzheimer's disease and vascular cognitive disorders: A review of mechanisms. *Oxid Med Cell Longev* **2022**, 6080282.

[24] Lin CJ, Yeh ML, Wu SF, Chung YC, Lee JC (2022) Acupuncture-related treatments improve cognitive and physical functions in Alzheimer's disease: A systematic review and meta-analysis of randomized controlled trials. *Clin Rehabil* **36**, 609-635.

[25] Warren A (2023) An integrative approach to dementia care. *Front Aging* **4**, 1143408.

[26] Yin W, Lv G, Li C, Sun J (2021) Acupuncture therapy for Alzheimer's disease: The effectiveness and potential mechanisms. *Anat Rec (Hoboken)* **304**, 2397-2411.

[27] Zhan Y, Fu Q, Pei J, Fan M, Yu Q, Guo M, Zhou H, Wang T, Wang L, Chen Y (2022) Modulation of brain activity and functional connectivity by acupuncture combined with donepezil on mild-to-moderate Alzheimer's disease: A neuroimaging pilot study. *Front Neurol* **13**, 912923.

[28] Zhou R, Xiao L, Xiao W, Yi Y, Wen H, Wang H (2022) Bibliometric review of 1992-2022 publications on acupuncture for cognitive impairment. *Front Neurol* **13**, 1006830.

[29] Wu L, Dong Y, Zhu C, Chen Y (2023) Effect and mechanism of acupuncture on Alzheimer's disease: A review. *Front Aging Neurosci* **15**, 1035376.

[30] Kan B, Dong Z, Tang Z, Zhao L, Li Z (2023) Acupuncture improves synaptic plasticity of SAMP8 mice through the RhoA/ROCK pathway. *Curr Alzheimer Res* **31**, 409-421.

[31] Wang Y, Zheng A, Yang H, Wang Q, Ren B, Guo T, Qiang J, Cao H, Gao YJ, Xu L, Li H, He L, Liu ZB (2021) "Olfactory three-needle" acupuncture enhances synaptic function in Aβ(1-42)-induced Alzheimer's disease via activating PI3K/AKT/GSK-3β signaling pathway. *J Integr Neurosci* **20**, 55-65.

[32] Li L, Li J, Dai Y, Yang M, Liang S, Wang Z, Liu W, Chen L, Tao J (2021) Electro-acupuncture improve the early pattern separation in Alzheimer's disease mice via basal forebrain-hippocampus cholinergic neural circuit. *Front Aging Neurosci* **13**, 770948.

[33] Yang Q, Zhu S, Xu J, Tang C, Wu K, Wu Y, Wang Y, Sheng H (2019) Effect of the electro-acupuncture on senile plaques and its formation in APP(+)/PS1(+) double transgenic mice. *Genes Dis* **6**, 282-289.

[34] Zhang X, Wei YT, Wang JY, Liu HX, Zhu TT, Yan XK (2023) [Effects of Yizhi Tiaoshen acupuncture on learning and memory function and the expression of phosphorylated tau protein in the hippocampus of Alzheimer's disease model rats]. *Zhongguo Zhen Jiu* **43**, 793-799.

[35] Xu A, Zeng Q, Tang Y, Wang X, Yuan X, Zhou Y, Li Z (2020) Electroacupuncture protects cognition by regulating tau phosphorylation and glucose metabolism via the AKT/GSK3β signaling pathway in Alzheimer's disease model mice. *Front Neurosci* **14**, 585476.

[36] Yang Y, Hu S, Lin H, He J, Tang C (2020) Electroacupuncture at GV24 and bilateral GB13 improves cognitive ability via influences the levels of Aβ, p-tau (s396) and p-tau (s404) in the hippocampus of Alzheimer's disease model rats. *Neuroreport* **31**, 1072-1083.

[37] Zheng X, Lin W, Jiang Y, Lu K, Wei W, Huo Q, Cui S, Yang X, Li M, Xu N, Tang C, Song JX (2021) Electroacupuncture ameliorates beta-amyloid pathology and cognitive impairment in Alzheimer disease via a novel mechanism involving activation of TFEB (transcription factor EB). *Autophagy* **17**, 3833-3847.

[38] Li L, Li L, Zhang J, Huang S, Liu W, Wang Z, Liang S, Tao J, Chen L (2020) Disease stage-associated alterations in learning and memory through the electroacupuncture modulation of the cortical microglial M1/M2 polarization in mice with Alzheimer's disease. *Neural Plast* **2020**, 8836173.

[39] Li Y, Jiang J, Tang Q, Tian H, Wang S, Wang Z, Liu H, Yang J, Ren J (2020) Microglia TREM2: A potential role in the mechanism of action of electroacupuncture in an Alzheimer's disease animal model. *Neural Plast* **2020**, 8867547.

[40] Ni H, Ren J, Wang Q, Li X, Wu Y, Liu D, Wang J (2023) Electroacupuncture at ST 36 ameliorates cognitive impairment and beta-amyloid pathology by inhibiting NLRP3 inflammasome activation in an Alzheimer's disease animal model. *Heliyon* **9**, e16755.

[41] Wu G, Li L, Li HM, Zeng Y, Wu WC (2017) Electroacupuncture ameliorates spatial learning and memory impairment via attenuating NOX2-related oxidative stress in a rat model of Alzheimer's disease induced by Aβ1-42. *Cell Mol Biol (Noisy-le-grand)* **63**, 38-45.

[42] Huang TI, Hsieh CL (2021) Effects of acupuncture on oxidative stress amelioration via Nrf2/ARE-related pathways in Alzheimer and Parkinson diseases. *Evid Based Complement Alternat Med* **2021**, 6624976.

[43] Lin YK, Liao HY, Watson K, Yeh TP, Chen IH (2023) Acupressure improves cognition and quality of life among older adults with cognitive disorders in long-term care settings: A clustered randomized controlled trial. *J Am Med Dir Assoc* **24**, 548-554.

[44] Song ZS, Li Z, Wang Y, Li MX, Liu Q, Shi KJ, Yao XW, Ding H, Li SL, Tang W (2023) [Mechanisms of moxibustion preconditioning underlying improving learning-memory ability by regulating polarization of microglia via TLR4/NF-κB signaling pathway in AD rats]. *Zhen Ci Yan Jiu* **48**, 525-532.

[45] Liao DM, Pang F, Zhou M, Li Y, Yang YH, Guo X, Tang CL (2022) [Effect of electroacupuncture on cognitive impairment in APP/PS1 mice based on TLR4/NF-κB/NLRP3 pathway]. *Zhen Ci Yan Jiu* **47**, 565-572.

[46] Xiao M, Wang XS, He C, Huang ZS, Chen HR, Kong LH (2023) The gut-brain axis: Effect of electroacupuncture pretreatment on learning, memory, and JNK signaling in D-galactose-induced AD-like rats. *Iran J Basic Med Sci* **26**, 532-539.

[47] Jiang Y, Lin Y, Tan Y, Shen X, Liao M, Wang H, Lu N, Han F, Xu N, Tang C, Song J, Tao R (2023) Electroacupuncture ameliorates cerebrovascular impairment in Alzheimer's disease mice via melatonin signaling. *CNS Neurosci Ther* **29**, 917-931.

[48] Wang Y, Zhao L, Shi HY, Jia YJ, Kan BH (2021) [RhoA/ROCK pathway involved in effects of Sanjiao acupuncture on learning and memory and synaptic plasticity in Alzheimer's disease mice]. *Zhen Ci Yan Jiu* **46**, 635-641.

[49] Wei TH, Hsieh CL (2020) Effect of acupuncture on the p38 signaling pathway in several nervous system diseases: A systematic review. *Int J Mol Sci* **21**, 4693.

[50] Hao X, Ding N, Zhang Y, Yang Y, Zhao Y, Zhao J, Li Y, Li Z (2022) Benign regulation of the gut microbiota: The possible mechanism through which the beneficial effects of manual

acupuncture on cognitive ability and intestinal mucosal barrier function occur in APP/PS1 mice. *Front Neurosci* **16**, 960026.

[51] Zhang Y, Ding N, Hao X, Zhao J, Zhao Y, Li Y, Li Z (2022) Manual acupuncture benignly regulates blood-brain barrier disruption and reduces lipopolysaccharide loading and systemic inflammation, possibly by adjusting the gut microbiota. *Front Aging Neurosci* **14**, 1018371.

[52] Jiang J, Liu H, Wang Z, Tian H, Wang S, Yang J, Ren J (2021) Electroacupuncture could balance the gut microbiota and improve the learning and memory abilities of Alzheimer's disease animal model. *PLoS One* **16**, e0259530.

[53] Ke C, Shan S, Fang C, Xia Y, Zhang W (2022) A review on characteristics of experimental research on acupuncture treatment for Alzheimer's disease: Study design. *Evid Based Complement Alternat Med* **2022**, 8243704.

[54] Park S, Lee JH, Yang EJ (2017) Effects of acupuncture on Alzheimer's disease in animal-based research. *Evid Based Complement Alternat Med* **2017**, 6512520.

[55] Chen RX, Huang XB, Xie DY, Li HY (2022) [Discussion of novel mode of acupuncture and moxibustion based on identifying the acupoint sensitization]. *Zhongguo Zhen Jiu* **42**, 665-668.

[56] Wang X, Li X, Gao Y, Wang D, Liu J, Fan X, Chen H, Zuo G, Li H, Zheng X, Zhang X, Zhang J, She Y (2023) Knowledge mapping of acupoint sensitization and acupoint specificity: A bibliometric analysis. *Front Neurosci* **17**, 1292478.

[57] Jiao S (2020) Biomedical optical imaging technology and applications: From basic research toward clinical diagnosis. *Exp Biol Med (Maywood)* **245**, 269-272.

[58] John S, Hester S, Basij M, Paul A, Xavierselvan M, Mehrmohammadi M, Mallidi S (2023) Niche preclinical and clinical applications of photoacoustic imaging with endogenous contrast. *Photoacoustics* **32**, 100533.

[59] Mirg S, Turner KL, Chen H, Drew PJ, Kothapalli SR (2022) Photoacoustic imaging for microcirculation. *Microcirculation* **29**, e12776.

[60] Sun Y, Ding F, Chen Z, Zhang R, Li C, Xu Y, Zhang Y, Ni R, Li X, Yang G, Sun Y, Stang PJ (2019) Melanin-dot-mediated delivery of metallacycle for NIR-II/photoacoustic dual-modal imaging-guided chemo-photothermal synergistic therapy. *Proc Natl Acad Sci U S A* **116**, 16729-16735.

[61] Manwar R, Gelovani JG, Avanaki K (2023) Bilirubin-biliverdin concentration measurement using photoacoustic spectroscopic analysis for determining hemorrhage age. *J Biophotonics* **16**, e202200316.

[62] Dasa MK, Markos C, Maria M, Petersen CR, Moselund PM, Bang O (2018) High-pulse energy supercontinuum laser for high-resolution spectroscopic photoacoustic imaging of lipids in the 1650-1850nm region. *Biomed Opt Express* **9**, 1762-1770.

[63] Dasa MK, Nteroli G, Bowen P, Messa G, Feng Y, Petersen CR, Koutsikou S, Bondu M, Moselund PM, Podoleanu A, Bradu A, Markos C, Bang O (2020) All-fibre supercontinuum laser for *in vivo* multispectral photoacoustic microscopy of lipids in the extended near-infrared region. *Photoacoustics* **18**, 100163.

[64] Lee H, Seeger MR, Lippok N, Nadkarni SK, van Soest G, Bouma BE (2022) Nanosecond SRS fiber amplifier for label-free near-infrared photoacoustic microscopy of lipids. *Photoacoustics* **25**, 100331.

[65] Cheng JX (2022) New "HOPE" laser for photoacoustic imaging of water. *Light Sci Appl* **11**, 107.

[66] Gu Y, Sun Y, Wang X, Li H, Qiu J, Lu W (2023) Application of photoacoustic computed tomography in biomedical imaging: A literature review. *Bioeng Transl Med* **8**, e10419.

[67] Jung U, Ryu J, Choi H (2022) Optical light sources and wavelengths within the visible and near-infrared range using photoacoustic effects for biomedical applications. *Biosensors (Basel)* **12**, 1154.

[68] Moothanchery M, Bi R, Kim JY, Balasundaram G, Kim C, Olivo M (2019) High-speed simultaneous multiscale photoacoustic microscopy. *J Biomed Opt* **24**, 1-7.

[69] Baik JW, Kim JY, Cho S, Choi S, Kim J, Kim C (2020) Super wide-field photoacoustic microscopy of animals and humans *in vivo*. *IEEE Trans Med Imaging* **39**, 975-984.

[70] Karlas A, Fasoula NA, Paul-Yuan K, Reber J, Kallmayer M, Bozhko D, Seeger M, Eckstein HH, Wildgruber M, Ntziachristos V (2019) Cardiovascular optoacoustics: From mice to men - A review. *Photoacoustics* **14**, 19-30.

[71] Setia A, Mehata AK, Priya V, Pawde DM, Jain D, Mahto SK, Muthu MS (2023) Current advances in nanotheranostics for molecular imaging and therapy of cardiovascular disorders. *Mol Pharm* **20**, 4922-4941.

[72] Chen Y, Chen B, Yu T, Yin L, Sun M, He W, Ma C (2021) Photoacoustic mouse brain imaging using an optical Fabry-Pérot interferometric ultrasound sensor. *Front Neurosci* **15**, 672788.

[73] Sciortino VM, Tran A, Sun N, Cao R, Sun T, Sun YY, Yan P, Zhong F, Zhou Y, Kuan CY, Lee JM, Hu S (2021) Longitudinal cortex-wide monitoring of cerebral hemodynamics and oxygen metabolism in awake mice using multi-parametric photoacoustic microscopy. *J Cereb Blood Flow Metab* **41**, 3187-3199.

[74] Kamali A, Dieckhaus LA, Peters EC, Preszler CA, Witte RS, Pires PW, Hutchinson EB, Laksari K (2023) Ultrasound, photoacoustic, and magnetic resonance imaging to study hyperacute pathophysiology of traumatic and vascular brain injury. *J Neuroimaging* **33**, 534-546.

[75] Sun W, Cai B, Rao J, Zhou F (2023) Characterization of cerebrovascular changes in mice treated with alcohol by photoacoustic imaging. *J Biophotonics* **16**, e202300038.

[76] Qiu T, Lan Y, Gao W, Zhou M, Liu S, Huang W, Zeng S, Pathak JL, Yang B, Zhang J (2021) Photoacoustic imaging as a highly efficient and precise imaging strategy for the evaluation of brain diseases. *Quant Imaging Med Surg* **11**, 2169-2186.

[77] Ma H, Wang Z, Cheng Z, He G, Feng T, Zuo C, Qiu H (2022) Multiscale confocal photoacoustic dermoscopy to evaluate skin health. *Quant Imaging Med Surg* **12**, 2696-2708.

[78] Wang Z, Yang F, Ma H, Cheng Z, Zhang W, Xiong K, Shen T, Yang S (2022) Bifocal 532/1064 nm alternately illuminated photoacoustic microscopy for capturing deep vascular morphology in human skin. *J Eur Acad Dermatol Venereol* **36**, 51-59.

[79] Wang Z, Yang F, Zhang W, Yang S (2022) Quantitative and anatomical imaging of human skin by noninvasive photoacoustic dermoscopy. *Bio Protoc* **12**, e4372.

[80] Lin L, Wang LV (2022) The emerging role of photoacoustic imaging in clinical oncology. *Nat Rev Clin Oncol* **19**, 365-384.

[81] Jo J, Folz J, Gonzalez ME, Paolì A, Eido A, Salfi E, Tekula S, Andò S, Caruso R, Kleer CG, Wang X, Kopelman R (2023) Personalized oncology by *in vivo* chemical imaging: Photoacoustic mapping of tumor oxygen predicts radiotherapy efficacy. *ACS Nano* **17**, 4396-4403.

[82] Lee MC, Landers K, Chan J (2023) Activity-based photoacoustic probes for detection of disease biomarkers beyond oncology. *ACS Bio Med Chem Au* **3**, 223-232.

[83] Privitera L, Musleh L, Paraboschi I, Ogunlade O, Ogunbiyi O, Hutchinson JC, Sebire N, Beard P, Giuliani S (2023) Dynamic changes in microvascular density can predict viable and non-viable areas in high-risk neuroblastoma. *Cancers (Basel)* **15**, 917.

[84] Ding N, Liu X, Chen N, Jiang J, Zhao H, Li Z, Zhang J, Liu C (2019) Lack of association between acupoint sensitization and microcirculatory structural changes in a mouse model of knee osteoarthritis: A pilot study. *J Biophotonics* **12**, e201800458.